

Influence of the Carbon/Anode Interaction on Direct Carbon Conversion in a SOFC

P. Desclaux¹, H.C. Schirmer¹, M. Woiton², E. Stern², M. Rzepka^{1,*}

¹ ZAE Bayern, Division 1, Walther-Meißner-Str. 6, 85748 Garching, Germany

² ZAE Bayern, Division 3, Haberstr. 2a, 91058 Erlangen, Germany

*E-mail: rzepka@muc.zae-bayern.de

Received: 19 April 2013 / Accepted: 31 May 2013 / Published: 1 July 2013

The influence of the physical and chemical fuel properties on the performance of a direct carbon fuel cell, based on a SOFC (solid oxide fuel cell) system, is tested at 850 °C. Using six different carbon samples, the experimental results show a clear dependence of both open circuit voltage (OCV) and maximum power density. This second parameter is dependent on the internal structure of the carbon material, such as particle size, specific surface area and degree of crystallinity. Moreover a variation of the force, pressing the carbon film against the anode layer, results in a reproducible variation of the OCV showing that the density of contact points with the active carbon atoms governs the electrochemical performance of a solid fuel / solid anode DCFC.

Keywords: DCFC, SOFC, carbon conversion, carbon/anode interaction, carbon activity.

1. INTRODUCTION

Utilization of carbon in high temperature fuel cells offers at medium term the possibility to directly convert the chemical energy of carbon materials into electricity. This fuel can be particularly suitable due to its abundant amount and because solid carbon-based materials are easy to store as well as to transport. Carbon fuel is present in different forms, such as hard coal, charcoal or carbonized biomass. In addition, as the main product at the anode is carbon dioxide it makes sequestration easy. Therefore, a negative carbon dioxide balance is even possible if the fuel materials are derived from biomass [1].

Moreover, the thermodynamic efficiency of a direct carbon fuel cell (DCFC) slightly exceeds 100% in a wide temperature range due to the positive near-zero value of the entropy change of the main reaction (Eq. 1).

In the last decades, different DCFC concepts have been developed by several research groups. They are classified according to the employed electrolyte type as follows [2,3]: two possible liquid salt electrolytes (molten carbonate [4] or molten hydroxide [5]) and a solid oxide electrolyte (ceramic layer) [6,7]. Recently, also combined technologies have been developed and investigated [8-13].

In this work, direct carbon conversion is studied in a solid oxide fuel cell. In principle, four different reactions can be involved in the overall anode process. Three of them are electrochemical oxidation reactions (four and two electron process, respectively), whereas the reverse Boudouard reaction is a purely chemical reaction (Eq. 4) [5, 8, 12]:



In this paper we study the influence of the fuel properties on the cell performance. Button cells without any additional anode layers are used in the experimental setup to investigate the direct conversion of carbon. Under these conditions, Eq. (3) should be negligible due to the non-porous surface of the YSZ electrolyte, in accordance to the experimental results of Nürnberger et al. [6].

2. EXPERIMENTAL

The DCFC experimental setup, based on a SOFC system, is shown in figure 1. The system is maintained at 850 °C using a tubular furnace. The oxide ceramic cells are electrolyte-supported and have a planar design. The cell is placed in a ceramic holder on a porous disc of sintered metal (Hastelloy X®) at the cathode side. The anode chamber is sealed by pressing the smooth-polished surface of a glass ceramic tube (Macor®) against the electrolyte layer with a contact pressure of about 0.17 Nmm⁻². In addition, a nitrogen flow rate of 300 mLmin⁻¹ is applied to remove minimal concentrations of the residual gas in the anode chamber. The carbon sample is introduced from the top through the internal alumina tube up to the surface of the cell. For that, a thin layer of carbon powder (approx. 500 µm) is pressed against a porous disc of Hastelloy X® (diameter of 9 mm). 15 to 30 mg are used for each sample, depending of the carbon material with a porosity of about 70 %. The cell is contacted at both sides with a platinum mesh. At the bottom side, the mesh is located on the porous disc of sintered metal and is directly in contact with the cathode layer. In the anode chamber, the current is collected through the carbon sample, using the electronic conductivity of the fuel. The contact pressure applied between the carbon fuel and the cell can be controlled by an external spring system. Typically, 0.27 Nmm⁻² are applied.

The solid oxide cells consist of a commercial cathode half cell, delivered by H. C. Starck Ceramics GmbH & Co. KG (type ESC2). The electrolyte of zirconia stabilized with 3 mol% of yttrium (3YSZ) has a thickness of about 90 µm and a diameter of 4 cm. The standard cathode layer is composed of 8YSZ and a mixture of lanthanum strontium manganese oxide (LSM) with a thickness of about 35 µm.

Six different carbon fuels are used in this work, which differ in morphology, particle size and degree of crystallinity. In advance, they have been analyzed using TEM, EDX, XRD and the BET method. Their properties are presented in Table 1. All the samples show a very high carbon content from 96 to more than 99 %. Traces of sulfur, silicate and aluminum have been detected, which are usual impurities in high carbon-based materials, partly because of their fabrication processes. Samples no. 1 and 2 are both carbon blacks: Printex® XE2-B (Evonik Degussa GmbH) and Vulcan® XC72 (Cabot Corporation). An active carbon powder of graphite containing nanoparticles (SGL Carbon), as well as carbon nanotubes (MER Corporation) have also been tested (samples no. 3 and 4, respectively). In addition, two graphitic powders were measured (samples no. 5 and 6). ECOPHIT® GFG 50M and TIMREX® KS10 have been provided by SGL Carbon and Timcal Group, respectively. Samples 1 to 4 show nanometric particles, whereas the particle size of both graphitic samples are in the range of some micrometers. Moreover, high specific surface areas were measured for the active carbon black “Printex® XE2-B” (up to $1000 \text{ m}^2\text{g}^{-1}$) as well as both materials “Vulcan® XC72” and “graphite nanopowder” ($220\text{--}250 \text{ m}^2\text{g}^{-1}$). On the contrary, the specific surface area of the other samples is very poor (not exceeding $40 \text{ m}^2\text{g}^{-1}$). By the XRD analysis, it has been found that the graphitic samples (no. 3, 5 and 6) show a very high degree of crystallinity. This is in contrast to both carbon blacks and the nanotube powder (samples 1, 2 and 4, respectively) which show the structure of amorphous carbon.

A potentiostat “Autolab PGSTAT 302N” by Deutsche METROHM GmbH & Co. KG was used to measure both current and voltage of the cell, as well as to perform electrochemical impedance spectroscopy (EIS). The current-voltage characteristics were obtained potentiostatically by applying a constant voltage value in the system and taking the current value after stabilization of the system (about 10 s) for each potential step. Applying different external pressures, the measured values of open circuit voltage (OCV) were stable within $\pm 0.01 \text{ V}$. The EIS measurements were performed over the frequency range of 0.1 MHz to 1 mHz at a potential corresponding of the OCV value.

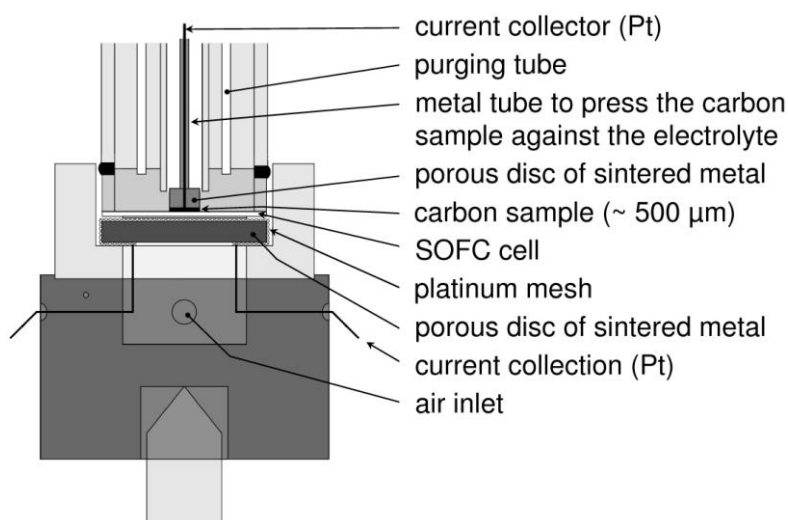


Figure 1. Experimental DCFC setup at ZAE Bayern. The fuel supply system, consisting of a current collector, a metal tube and a porous disc with the attached carbon sample, is movable and can be introduced from the top.

Table 1. Physical and chemical properties of the different used carbon materials.

sample no.	sample	carbon type	particle size μm	particle / form	impurity content / wt. %	crystallinity parameters (rank)	specific surface area / m^2g^{-1}
1	Printex® XE2-B	channel black	0.03 - 0.035	spherical	Si (0.36) S (0.49)	5	974
2	Vulcan® XC72	furnace carbon black	0.02 - 0.1	spherical	Si (1.47)	6	223
3	graphite nanopowder	active carbon	0.05 - 0.2	lamellar	S (4.41)	1	251
4	nanotubes	carbon nanotubes	\varnothing 0.08 $l > 1$	“spaghetti”-like	Si (0.29)	4	36
5	ECOPHIT® GFG 50M	graphitic powder	40 - 60	lamellar	S (3.54) Si (0.79) Al (0.34)	2	20
6	TIMREX® KS10	graphitic powder	6 - 12	lamellar	Si (0.03)	3	10

3. RESULTS

Measurements of I-V curves were performed for all carbon materials (see Table 1) at an operating temperature of 850 °C. In Fig. 2 the results are shown after I-R correction with the ohmic resistivity, determined for each sample by electrochemical impedance spectroscopy. As can be seen the OCV value and the maximum current density strongly depend on the carbon properties. Both carbon black materials (Printex® XE2-B as well as Vulcan® XC72) show outstanding performance in comparison to the other samples, which are displayed in a larger magnification in Fig. 3. The measured current densities are only located in the range of 0 to 4 mAcm^{-2} .

All graphitic materials (ECOPHIT® GFG 50M, TIMREX® KS10 and graphite nanopowder) show poor cell performance as well as low open circuit voltage. As crystalline carbon materials are mostly composed of planar-organized hexagonal graphite sheets, less contact of reactive carbon atoms is possible with the active surface at the anode side of the electrolyte layer compared to samples having an amorphous internal structure. Additionally, small particles allow to increase the active surface area of the fuel. Using the carbon material “graphite nanopowder” (sample no. 3), the low cell performance in spite of its high specific surface area attests that the main factors influencing the electrochemical reactivity are both degree of crystallinity and particle size. Moreover, nanotubes might not be suitable for this application and the electrochemical reactivity of this sample is dramatically low. The samples with the best performances are amorphous carbon powders, containing particles in the nanometric scale (20 to 100 nm) and high specific surface areas (220 to 1000 m^2g^{-1}).

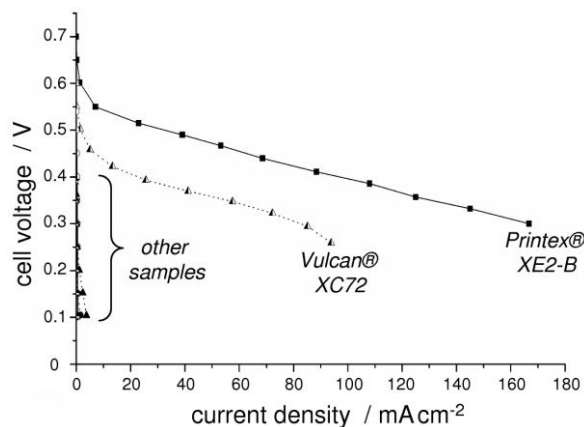


Figure 2. I-V curves of the YSZ-based cells operating at 850 °C with the six different carbon samples; gas flow rates: 300 mLmin⁻¹ of nitrogen and 150 mLmin⁻¹ of synthetic air.

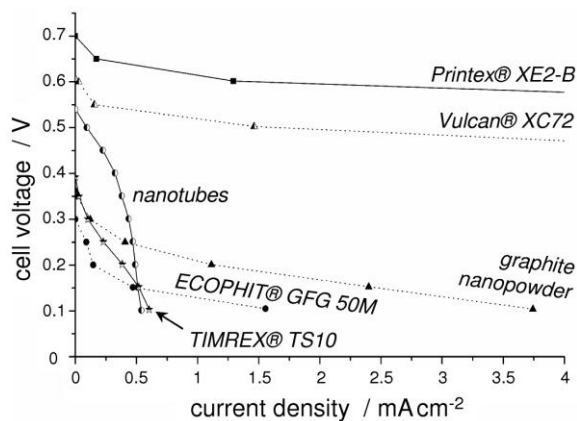


Figure 3. Data of Fig. 2 for a current density range of 0 to 4 mAcm⁻².

In Fig. 3, the measured values of the open circuit voltage are much lower than the thermodynamic equilibrium voltage for standard concentrations (1.03 V for the complete oxidation of carbon). Moreover, the OCV value depends on the carbon material. For each sample (no. 1 to 6) following values were obtained: 0.70, 0.61, 0.36, 0.54, 0.30 and 0.40 V, respectively. This may be attributed to the special case of the electrochemical carbon/anode interaction which influences the effective carbon activity by providing only single isolated contact points. This will be discussed in more detail in section 4.

During the electrochemical conversion of the solid carbon, oxygen ions delivered by the electrolyte at the anode side must be in close contact with reactive sites of the fuel (two-phase boundary). In order to enhance the number of contact points at the reactive interface (solid anode / solid fuel) a constant external pressure of 0.27 Nmm⁻² was applied during the measurements on the sample. In addition, this increases the electronic conductivity of the carbon fuel by minimizing the bulk contact resistance between the carbon particles. In order to test the influence of the contact pressure on the OCV value, this parameter has been varied using the carbon material “Vulcan® XC72”. The experimental data are presented in Fig. 4 for an operating temperature of 850 °C. A

distinct increase of the OCV value from 0.61 to 0.66 V is observable for external pressures between 0 and 0.66 Nmm⁻². A plateau value of about 0.65 V is reached for pressures over 0.27 Nmm⁻². Thus, the external pressure applied on the sample significantly influences the value of the open circuit voltage.

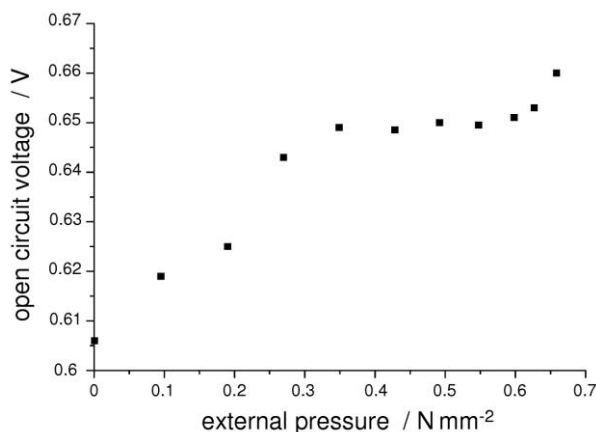


Figure 4. Influence of the external pressure, applied on the sample, on the measured value of the open circuit voltage; used carbon fuel: Vulcan® XC72; operating temperature: 850 °C; gas flow rates: 300 mLmin⁻¹ of nitrogen and 150 mLmin⁻¹ of synthetic air.

4. DISCUSSION

As stated in the introduction, the carbon oxidation can occur in a single direct oxidation process or in a two step process via the reverse Boudouard reaction followed by a subsequent electrochemical conversion of CO at the anode. However, this latter process may be strongly suppressed due to the smooth non-porous anode. This is confirmed by the experimental results given in [6]. Moreover, the strong dependence of the cell performance on the sample properties (see Fig. 3) shows that the reaction step involving the carbon fuel is the rate-determining step. On the other side, the reverse Boudouard reaction takes place on a large surface area where carbon dioxide is in contact with the three-dimensional structure of the porous carbon fuel, giving some evidence that this is not the rate-determining step compared to the subsequent CO oxidation on the flat anode. Therefore, the strong dependence of the cell performance on the carbon properties shows that the direct oxidation of the solid carbon material dominates the overall process at the anode.

In the thermodynamic equilibrium, a good approximation of the open circuit potential for partial and complete carbon oxidations can be given by the Nernst equations:

$$\Delta U_{0,C \rightarrow CO_2}(T) = \Delta U_0^\theta C \rightarrow CO_2(T) + \frac{RT}{4F} \cdot \ln \left(a_C \cdot \frac{p_{O_2}}{p_{CO_2}} \right) \quad (5)$$

$$\Delta U_{0,C \rightarrow CO}(T) = \Delta U_0^\theta C \rightarrow CO(T) + \frac{RT}{2F} \cdot \ln \left(a_C \cdot \frac{p_{O_2}^{0.5}}{p_{CO}} \right) \quad (6)$$

with p_{O_2} , p_{CO_2} and p_{CO} the respective partial pressure (in units of $p^\theta = 1$ bar) of the involved gaseous species and $\Delta U_0^\theta(T)$ the thermodynamic standard voltage. From the thermodynamic data at

850 °C the associated values of the thermodynamic standard voltage are 1.03 and 1.09 V for Eqs. (5) and (6), respectively. In this work, the measured OCV values vary between 0.3 to 0.7 V, which is in accordance with the published values of other groups working on the same DCFC concept with utilization of carbon blacks as carbon fuel: about 0.7 V using “Vulcan XC72” [13,14] and approx. 0.78 V using “Printex® 90” by Evonik Degussa GmbH [15]. Therefore, there is some evidence that these low OCV values are no coincidence but should be attributed to the special characteristics of the analyzed system with a solid-solid contact at the interface carbon/anode. Usually, the carbon fuel is considered like a pure solid (ideal graphite) and its activity is taken as $a_C = 1$. Considering this activity value, the low measured OCV values can be hardly explained by the Nernst equations (5) or (6). This may be attributed to the fact that, in the point-like solid-solid contact, no equilibrium is established or that the electrochemical activity of the carbon fuel is lower than one, such as in the comparable situation of submonolayers of active materials [16].

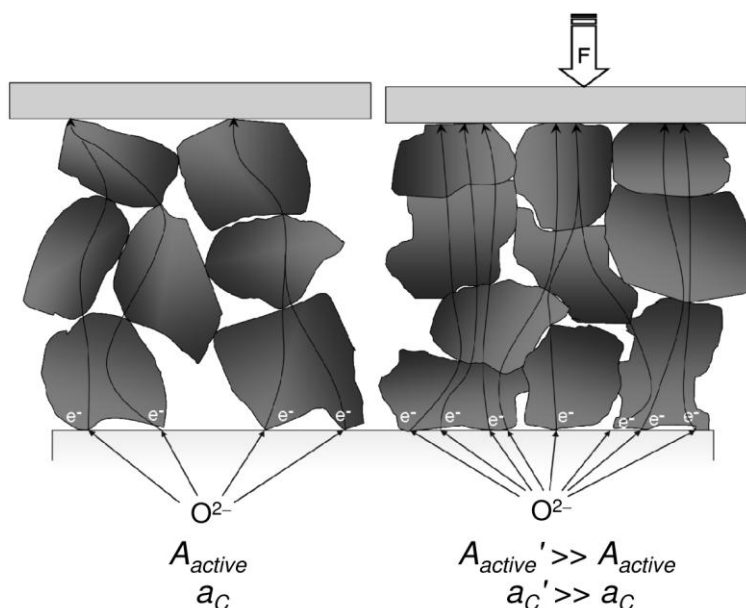


Figure 5. Schematic representation of the effect of an applied contact pressure on the carbon particles, leading to a higher contact surface with the anode and thus enhancing the carbon activity. In addition, the fuel material shows a better electronic conductivity and thus a higher current collection through the sample is possible.

In addition, as already described in section 3, the internal structure of the used carbon material also influences the value of the open circuit voltage (see Fig. 3). The OCV values of all graphitic carbon materials (samples no. 3, 5 and 6) are in the range of 0.3 to 0.4 V, whereas amorphous carbons (samples 1 and 2) show much higher OCV values between 0.61 and 0.7 V, respectively. This effect is qualitatively in accordance with the contact pressure dependence of the measured OCV variation, attesting that the number of active carbon atoms, which are present at the interface, may strongly depend on the carbon morphology as well as on the arrangement on the atoms with each other. Thus, highly ordered graphitic samples provide less reactive surface atoms than disordered amorphous materials.

5. CONCLUSIONS

In this work, it has been shown that the electrochemical performance of a DCFC, based on a SOFC system, strongly depends on the interaction between the carbon fuel and the anode. This is influenced by (i) the physical and chemical properties of the used material, such as degree of crystallinity, particle size or specific surface area, as well as by (ii) the force which is applied to press the carbon particles against the anode side of the electrolyte. Thus, the overall density of active carbon atoms in direct contact with the anode may play an important role, as it varies with both physical and chemical properties and can be externally influenced by increasing contact pressure between the carbon fuel film and the anode layer.

ACKNOWLEDGEMENT

The experimental work at ZAE Bayern has been financially supported by the Arbeitsgemeinschaft industrieller Forschungsvereinigungen „Otto von Guericke“ e.V (AiF) under grant number „IGF-Vorhaben 16507 N“, in the context of a development program of the Industrielle Gemeinschaftsforschung (IGF) from the Bundesministerium für Wirtschaft und Technologie in Germany.

References

1. P. Desclaux, S. Nürnberger and U. Stimming, in R. Steinberger-Wilckens and W. Lehnert (Eds.), *Innovations in Fuel Cell Technologies*, RSC Publishing, Cambridge, 2010, p. 190.
2. P. Desclaux, M. Rzepka, U. Stimming and R. Hempelmann, *J. Phys. Chem.* (2012) in press, DOI: 10.1524/zpch.2012.0253.
3. A. C. Rady, S. Giddey, S. P. S. Badwal, B. P. Ladewig and S. Bhattacharya, *Energy Fuels*, 26 (2012) 1471.
4. N. J. Cherepy, R. Krueger, K.J. Fiet, A. F. Jankowski and J. F. Cooper, *J. Electrochem. Soc.*, 152 (2005) A80.
5. S. Zecevic, E. M. Patton and P. Parhami, *Carbon*, 42 (2004) 1983.
6. S. Nürnberger, R. Bußar, P. Desclaux, B. Franke, M. Rzepka and U. Stimming, *Energy Environ. Sci.*, 3 (2010) 150.
7. R. Z. Liu, C. H. Zhao, J. L. Li, F. R. Zeng, S. R. Wang, T. L. Wen and Z. Y. Wen, *J. Power Sources*, 195 (2010) 480.
8. D. Cao, Y. Sun and G. Wang, *J. Power Sources*, 167 (2007) 250.
9. T. M. Gür, M. Homel and A. V. Virkar, *J. Power Sources*, 195 (2010) 1085.
10. T. Tao, M. Koslowske, J. Brodie and J. Bentley, Abstract #472, 220th ESC Meeting, Boston, MA, USA, Oct. 9-14, 2011.
11. K. Hemmes and M. Cassir, in proceedings *Second International Conference on Fuel Cell Science, Engineering and Technology*, ASME, Rochester, NY, USA, June 14-16, 2004, p. 395.
12. S. L. Jain, Y. Nabae, B. J. Lakeman, K. D. Pointon and J. T. S. Irvine, *Solid State Ion.*, 179 (2008) 1417.
13. C. R. Jiang and J. T. S. Irvine, *J. Power Sources*, 196 (2011) 7318.
14. A. Kulkarni, S. Giddey and S. P. S. Badwal, *Solid State Ion.*, 194 (2011) 46.
15. M. G. Werhahn, O. Schneider and U. Stimming, *ESC Trans.* (2013) in press.
16. J. Barbier, in G. Ertl, H. Knözinger, J. Weitkamp (Eds.), *Preparation of Solid Catalysts*, WILEY-VCH, Weinheim, 1999, pp. 526.